Experimental Estimation of Cooling Effect due to Blood Flow in a Thick Blood Vessel

#Atsushi HIROE [1], Kazuyuki SAITO [2], Masaharu TAKAHASHI [2], and Koichi ITO [3]
[1]*Graduate School of Science and Technology, Chiba University*
[2]*Research Center for Frontier Medical Engineering, Chiba University*
[3]*Faculty of Engineering, Chiba University*
1-33 Yayoi-cho, Inage-ku, Chiba 263-8522, Japan, hiroe@graduate.chiba-u.jp

Abstract

Hyperthermia is one of the modalities for cancer treatment, utilizing the difference of thermal sensitivity between tumor and normal tissues. Therefore, the most important point in the treatment of the hyperthermia is that the tumor is heated up to the therapeutic temperature, between 42 and 45 °C or more. Up to now, we have developed a coaxial-slot antenna for intracavitary microwave hyperthermia aiming at the treatment of the bile duct carcinoma. This antenna is inserted into the forceps channel of an endoscope and is led to the target tumor. Currently, there are thick blood vessels around the bile duct. Therefore, the cooling effect due to the thick blood vessels needs to be considered. In this paper, we investigated by measurement the cooling effect due to the blood flow in the thick blood vessel around the bile duct. At first, a tissue-equivalent solid phantom with a cylindrical hole of 20 mm in diameter was fabricated. The cooling effect of the thick blood vessel is realized by pouring a saline solution into the cylindrical hole. Then, the antenna is placed at a distance of 5 mm from the cylindrical hole. As a result, the heated region is observed around the tip of the antenna, although there is a thick blood vessel close to the antenna. Moreover, we confirmed the effectiveness of the proposed phantom by comparing the resultant temperature distributions by measurement and the ones obtained by calculation.

1. INTRODUCTION

In recent years, various types of medical applications of microwaves have widely been investigated and reported [1]. They are microwave hyperthermia [2], [3] and microwave coagulation therapy (MCT) [4], [5] for medical treatment of cancer, cardiac catheter ablation for ventricular arrhythmia treatment [6], [7], thermal treatment of benign prostatic hypertrophy (BPH) [8], [9], etc. Until now, the authors have been studying antennas for microwave hyperthermia. Hyperthermia is one of the modalities for cancer treatment, utilizing the difference of thermal sensitivity between tumor and normal tissues. In this treatment, the tumor is heated up to the therapeutic temperature, between 42 and 45 °C or more without overheating the surrounding normal tissues.

There are a few methods for heating the cancer cells inside the body. The authors have been especially studying the coaxial-slot antenna with endoscope [10], [11], which is one of the thin microwave antennas, for the interstitial microwave hyperthermia. As a result of these investigations, some cases of actual treatments were realized by use of our developed antenna, and the effectiveness of these treatments could be confirmed [11].

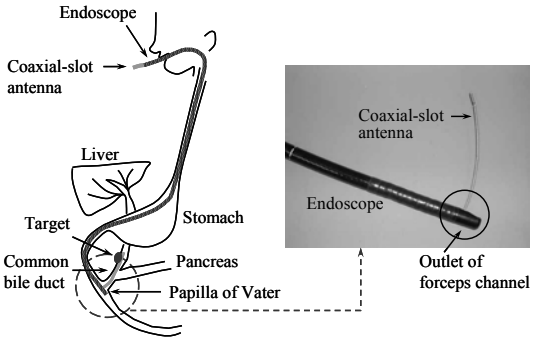

(a) Scheme of the treatment and tip of the endoscope with antenna

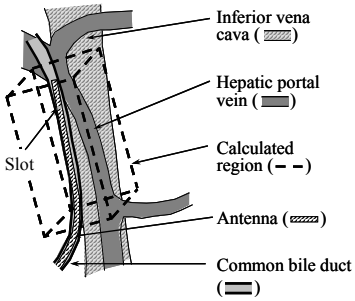

(b) Two main thick blood vessels around the common bile duct

Fig. 1: Bile Duct Treatment

This time we have developed a coaxial-slot antenna aiming at intracavitary heating for the bile duct carcinoma. Here, thick blood vessels lay near the bile duct. Therefore, we need to evaluate the cooling effect of the thick blood vessel placed near the antenna. Until now, the authors have been investigated the heating performances of this antenna by calculation with a simple model in the case of the cooling effect in the

thick blood vessel is considered. This time, we measured the heating region of this antenna by use of a dynamic phantom. This phantom includes a cylindrical hole in which a saline solution that simulates the cooling effect due to the thick blood vessel is poured.

In Section 2, the scheme of the treatment and the structure of the antenna are explained. In Section 3, the dynamic phantom used to simulate the cooling effect of the thick blood vessel and the procedure of numerical calculations are introduced. Moreover, the heat transfer coefficient of the boundary between the cylindrical hole and the phantom is calculated to evaluate the cooling effect due to the thick blood vessel. In Section 4, the procedure of calculation for temperature distributions around the bile duct to confirm the validity of measurement is shown. In Section 5, the measured and calculated temperature distributions are discussed. Finally, conclusions are presented in Section 6.

2. SCHEME OF THE TREATMENT AND STRUCTURE OF THE ANTENNA

Fig. 1(a) (left) shows the scheme of the treatment and the tip of the endoscope with the coaxial-slot antenna (right). In this treatment, the endoscope is first inserted into the duodenum, and a long and flexible coaxial-slot antenna is placed into the forceps channel of the endoscope, which is used to insert the tool for surgical treatment. Finally, the antenna is guided to the bile duct through the papilla of Vater, which is located in the duodenum, and the tip of the antenna is placed nearby the target.

Fig. 1(b) shows the two thick blood vessels (inferior vena cava and hepatic portal vein) around the common bile duct. Here, the most important point in the treatment of hyperthermia is that the target is heated up to more than the therapeutic temperature. As there are thick blood vessels around the bile duct as shown in Fig. 1(b), it is feared that a sufficient therapeutic region is not obtained, because of the cooling effect of these blood vessels. Therefore, it is needed to investigate the cooling effect due to these blood vessels.

Fig. 2 shows the structure of the proposed coaxial-slot antenna for the bile duct treatment. This antenna is made of a commercially available flexible coaxial cable, which is 1.8 mm in diameter. One ring slot is cut on the cable and the outer conductor and the tip of the cable is short-circuited. We confirmed that the fabricated prototype antenna can be inserted into the forceps channel without any problems. Here, the operating frequency is 2.45 GHz, which is one of the ISM (Industrial, Scientific and Medical) band.

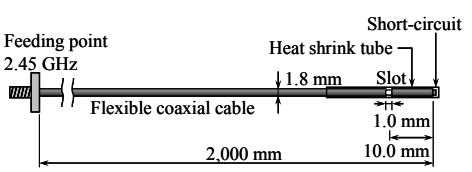

Fig. 2: A Coaxial-Slot Antenna for Intracavitary Microwave Hyperthermia

3. EXPERIMENTAL SYSTEM

A. Tissue Equivalent Solid Phantom

As shown in Fig. 1(a), this antenna will be strongly bent at the outlet of the forceps channel of the endoscope. In the previous experiment with a phantom, a high SAR region was observed only at the tip of the antenna, regardless of the bent angle. Therefore, it can be said we have only to analyze the tip of the antenna.

Fig. 3 shows the tissue equivalent solid phantom considering the cooling effect of the thick blood vessel. The phantom size is 150 × 150 × 150 mm^3. In this paper, only the blood vessel (hepatic portal vein) next to the bile duct is considered. The hepatic portal vein is modelled as a cylindrical hole of 20 mm in diameter. We can control the velocity of the saline solution by changing the diameter of a small hole etched on a rubber sheet placed at the bottom of the phantom. The distance between the hepatic portal vein and the antenna is 5 mm. Moreover, this phantom is divided into two portions; the upper and lower part of the observation plane.

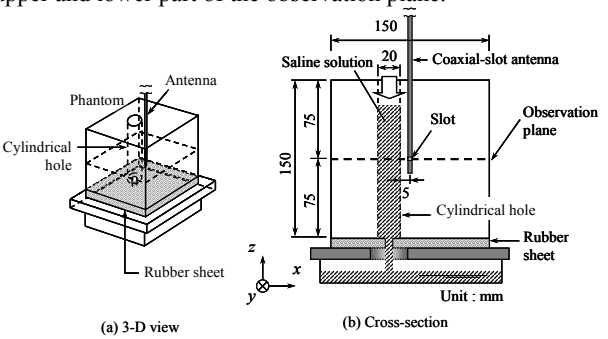

Fig. 3: Tissue Equivalent Solid Phantom

B. Procedure of measurement

First, the 0.35 % saline solution is poured into the cylindrical hole that models the hepatic portal vein. The value of the conductivity of the 0.35 % saline solution is 2.16 S/m, which is almost the same value that the human blood at 2.45 GHz. During the experiment, the saline solution is continuously poured. After heating, the upper part of the phantom is quickly removed, and then the exposed surface of the phantom is observed by an infrared camera.

The relative permittivity of this phantom is 47.0 and the conductivity is 2.21 S/m, which is equivalent to the electrical constants of human at 2.45 GHz. The heating time is 120 seconds, and the input power to the antenna is 33 W. Here, this antenna is made of a flexible and long coaxial cable, so we need to consider the loss of the input power. Therefore, the radiation power from the slot is estimated to be 10.3 W by calculation the cable loss and reflection loss of the antenna.

The initial temperature of the phantom and saline solution was almost the same. This phantom melts over approximately 60 ^{o}C, so we paid attention to the maximum temperature of the phantom during the measurement. Moreover, we conducted a measurement with a phantom which has no cylindri-

cal hole to compare the heating performances of the coaxial-slot antenna without the cooling effect.

C. Calculation of the heating transfer coefficient

In this section, we calculate the heat transfer coefficient between the saline solution and the phantom to evaluate the cooling effect due to a thick blood vessel from the following equation [12]:

$$h = Nu\kappa / D$$

where, Nu is the Nusselt number obtained by the following equations:

$$Nu = 4 + 0.48624\ln^2\left[\mathrm{Re}\times \mathrm{Pr}\times D/(18\times l)\right]$$
$$\mathrm{Re} = \rho VD / \mu$$

where, Pr is the Prandtl number (Pr = 7.001), and other parameters of these calculations are shown in table 1 (Table 1 includes the parameter of calculation which is introduced in the following section). These parameters are the value for water at 20 ^{o}C. In addition, D is the diameter and l is the length of the cylindrical hole (D = 20 mm, l = 150 mm). From these equations, h is calculated to be 1,575 W/m^2·K.

Here, h of the blood flow over the endocardium is approximately in the order of 1,000 ~ 2,000 W/m^2·K [13], [14]. Therefore, the value of the heating transfer coefficient in our model is enough, because the h of the hepatic portal vein is thought to be lower than the h of the blood flow over the endocardium.

TABLE 1: PARAMETERS OF TISSUES FOR NUMERICAL CALCULATION

	Phantom	Saline solution
Relative permittivity ε_r	47.0	79.7
Conductivity σ [S/m]	2.21	2.16
Density ρ [kg/m^3]	939	998
Specific heat c [J/kg·K]	3,600	4,200
Thermal conductivity κ [W/m·K]	0.55	0.60
Blood flow rate* F [m^3/kg·s]	0.0	0.0
Viscosity of saline solution μ [J/kg·K]	-	1.0×10^{-6}
Velocity** V [m/s]	-	0.021

* Flow rate of the capitally blood in the tissue
** Observed value

4. NUMERICAL CALCULATIONS

We have calculated the temperature distributions around the bile duct to confirm the validity of the results obtained by measurement.

First of all, we construct a calculation model and analyze the electric field around the antenna by the finite-difference time-domain (FDTD) method. The parameters for the FDTD calculation are shown in Table 2. Next, the specific absorption rate (SAR) is calculated by the following equation:

$$\mathrm{SAR} = \frac{\sigma}{\rho}E^2 \qquad [\mathrm{W/kg}]$$

where, E is electric field around the antenna [V/m], σ is the conductivity of the tissue [S/m] and ρ is the density of the tissue [kg/m^3].

Finally, we calculate the temperature distribution around the antenna. In order to obtain the temperature distribution in the tissue, we numerically analyze the bioheat transfer equation [13] including the obtained SAR values using the finite-difference method (FDM). The bioheat transfer equation is given by

$$\rho c\frac{\partial T}{\partial t} = \kappa\nabla^2 T - \rho\rho_c c_b F\left(T - T_b\right) + \rho\cdot\mathrm{SAR}$$

where T is the temperature of the tissue [^{o}C], t is the time [s], ρ_b is the density of the blood [kg/m^3], c_b is the specific heat of the blood [J/kg·K], T_b is the temperature of the blood [^{o}C], the other parameters for temperature calculation are shown in Table 1.

TABLE 2: PARAMETERS FOR FDTD CALCULATIONS

Cell size [mm] (minimum)	Δx, Δy Δz	0.05 1.0 (const.)
Cell size [mm] (maximum)	Δx, Δy Δz	1.0 1.0 (const.)
Absorbing boundary condition		Mur (1st. order)

5. TEMPERATURE DISTRIBUTIONS

Fig. 5 shows the temperature distributions in the observation plane, which is defined in Fig. 3. Figs. 5(a) and (b) represent the temperature distribution in the case the cooling effect of the thick blood vessel is considered and the case with no cooling effect, respectively. These results show temperature rise, which is obtained by subtracting the initial temperature of the phantom from the temperature after the measurement. The thick white line is a region more than 5 ^{o}C rise of temperature.

As shown in Fig. 5(a), the cooling effect of the saline solution is confirmed around the boundary of the phantom and the saline solution. Moreover, the thick white line in the positive region of x is almost the same when comparing Figs. 5(a) and (b). Therefore, it is confirmed that the cooling effect of the thick blood vessel appears only the surface.

The thick grey dotted line is a region more than 5 ^{o}C rise of temperature obtained by calculation. This line is in good agreement with the results of measurement (thick white line), so the validity of the experiment was confirmed. Moreover, the calculated temperature distributions is almost the same when the heat transfer coefficient is varied between 500 ~ 1,500 W/m^2·K. In addition, these results are in good agreement with the calculated temperature result when the temperature of blood vessel is equal to the initial temperature. From these results, the effectiveness of the proposed phantom is confirmed, and it can be said the phantom is helpful to evaluate the cooling effect due to the thick blood vessel as the hepatic portal vein around the common bile duct.

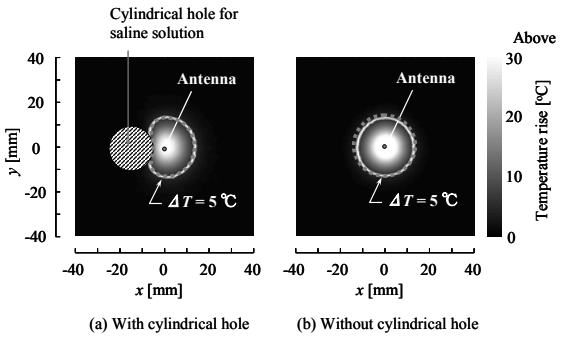

Fig. 5: Temperature Distributions

6. Conclusions

In this paper, we fabricated the phantom with cylindrical hole considering the cooling effect due to the thick blood vessel by pouring a saline solution into the hole. We experimentally evaluated the heating performances of a coaxial-slot antenna for intracavitary microwave hyperthermia aiming at the treatment of the bile duct carcinoma by conducting measurements with the proposed phantom. As a result, the heated region is observed around the tip of the antenna, although the thick blood vessel exists at 5 mm in distance with the antenna. Moreover, the effectiveness of this proposed phantom is confirmed to evaluate the cooling effect due to the thick blood vessel as the hepatic portal vein around the common bile duct. As a further study, we will fabricate a tissue-equivalent phantom which is able to simulate the cooling effect of capillarities of the tissue.

ACKNOWLEDGEMENT

The authors would like to thank Dr. Toshio Tsuyuguchi, Chiba University Hospital, Chiba, Japan for his valuable comments from the clinical side.

REFERENCES

[1] F. Sterzer, "Microwave medical devices," *IEEE Microwave Meg.*, vol. 3, no. 1, pp. 65-70, Mar. 2002.

[2] M. H. Seegenschmiedt, P. Fessenden, and C. C. Vernon, Eds., *Thermoradiotherapy and thermochemotherapy*, Berlin, Germany: Springer-Verlag, 1995.

[3] M. Converse, E. J. Bond, S. C. Hagness, and B. D. Van Veen, "Ultrawide-band microwave space-time beamforming for hyperthermia treatment of breast cancer: a computational feasibility study," *IEEE Trans. Microwave Theory Tech.*, vol. 52, pp. 1876-1889, Aug. 2004.

[4] T. Seki, M. Wakabayashi, T. Nakagawa, T. Itoh, T. Shiro, K. Kunieda, M. Sato, S. Uchiyama, and K. Inoue, "Ultrasonically guided percutaneous microwave coagulation therapy for small carcinoma," *Cancer*, vol. 74, no. 3, pp. 817-825, Aug. 1994.

[5] P. Liang, B. Dong, X. Yu, D. Yu, Z. Cheng, L. Su, J. Peng, Q. Nan, and H. Wang, "Computer-aided dynamic simulation of microwave-induced thermal distribution in coagulation of liver cancer," *IEEE Trans. Biomed. Eng.*, vol. 48, pp. 821-829, Jul. 2001.

[6] R. D. Nevels, G. D. Arndt, G. W. Raffoul, J. R. Carl, and A. Pacifico, "Microwave catheter design," *IEEE Trans. Biomed. Eng.*, vol. 45, pp. 885-890, Jul. 1998.

[7] P. Bernardi, M. Cavagnaro, J. C. Lin, S. Pisa, and E. Piuzzi, "Distribution of SAR and temperature elevation induced in a phantom by a microwave cardiac ablation catheter," *IEEE Trans. Microwave Theory Tech.*, vol. 52, pp. 1978-1986, Aug. 2004.

[8] D. Despretz, J. -C. Camart, C. Michel, J. -J. Fabre, B. Prevost, J. -P. Sozanski, and M. Chivé, "Microwave prostatic hyperthermia: interest of urethral and rectal applicators combination - Theoretical study and animal experimental results," *IEEE Trans. Microwave Theory Tech.*, vol. 44, pp. 1762-1768, Oct. 1996.

[9] A. Dietsch, J. -C. Camart, J. P. Sozanski, B. Prevost, B. Mauroy, and M. Chivé, "Microwave thermochemotherapy in the treatment of the bladder carcinoma - electromagnetic and dielectric studies - clinical protocol," *IEEE Trans. Biomed. Eng.*, vol. 47, pp. 633-641, May 2000.

[10] K. Ito, K. Ueno, M. Hyodo, and H. Kasai, "Interstitial applicator composed of coaxial ring slots for microwave hyperthermia,," in *Proc. Int. Antennas Propagation Symp.*, Tokyo, Japan, Aug. 1989, pp. 253-256.

[11] K. Saito, H. Yoshimura, K. Ito, Y. Aoyagi, and H. Horita, "Clinical trials of interstitial microwave hyperthermia by use of coaxial-slot antenna with two slots," *IEEE Trans. Microwave Theory Tech.*, vol. 52, pp. 1987-1991, Aug. 2004.

[12] C.X. Zhang, S. Zhang, Z. Zhang, and Y.Z. Chen, "Effects of large blood vessel locations during high intensity focused ultrasound therapy for hepatic tumors: a finite element study," in *Proc. IEEE Eng. in Med. and Biology 27th Annual Conf.*, Shanghai, China, Sep. 2005.

[13] Z. Kaouk, A. Khebir, and P. Savard, "A finite element model of a microwave catheter for cardiac ablation," *IEEE Trans. Microwave Theory Tech.*, vol. 44, pp. 1848-1854, Oct. 1996.

[14] S. Labonté, "A computer simulation of radio-frequency ablation of the endocardium," *IEEE Trans. Biomed. Eng.*, vol. 41, pp. 883-890, Sep. 1994.